CHAPTER 6

BASIC RADIATION DETECTORS

C.W.E. VAN EIJK
Faculty of Applied Sciences,
Delft University of Technology,
Delft, Netherlands

6.1. INTRODUCTION

6.1.1. Radiation detectors — complexity and relevance

Radiation detectors are of paramount importance in nuclear medicine. The detectors provide a wide range of information including the radiation dose of a laboratory worker and the positron emission tomography (PET) image of a patient. Consequently, detectors with strongly differing specifications are used. In this chapter, general aspects of detectors are discussed.

6.1.2. Interaction mechanisms, signal formation and detector type

A radiation detector is a sensor that upon interaction with radiation produces a signal that can preferably be processed electronically to give the requested information. The interaction mechanisms for X rays and γ rays are the photoelectric effect, Compton scattering and pair formation, where the relative importance depends on the radiation energy and the interaction medium. These processes result in the production of energetic electrons which eventually transfer their energy to the interaction medium by ionization and excitation. Charged particles, such as α particles, transfer their energy directly by ionization and excitation. In all cases, the ionization results either in the production of charge carriers, viz. electrons and ions in a gaseous detection medium, and electrons and holes in a semiconductor detector material, or in the emission of light quanta in a scintillator. These processes represent the three major groups of radiation detectors, i.e. gas filled, semiconductor and scintillation detectors. In the former two cases, a signal, charge or current is obtained from the detector as a consequence of the motion of charge in the applied electric field (Figs 6.1(a) and (b)). In the scintillation detector, light emission is observed by means of a light sensor that produces observable charge or current (Fig. 6.1(c)). A detailed discussion is presented in Sections 6.2–6.4.

6.1.3. Counting, current, integrating mode

In radiology and radiotherapy, radiation detectors are operated in current mode. The intensities are too high for individual counting of events. In nuclear medicine, on the contrary, counting mode is primarily used. Observing individual events has the advantage that energy and arrival time information are obtained, which would be lost in current mode. In the case of a personal dosimeter, the detector is used in integrating mode. The dose is, for example, measured monthly. Furthermore, instead of real time observation, the information is extracted at a much later time after the actual interaction.
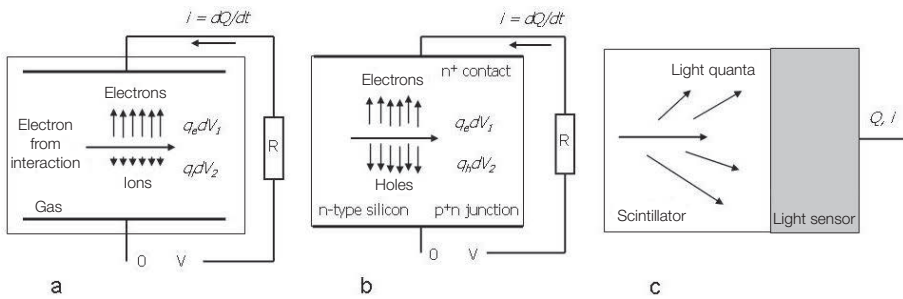

FIG. 6.1. Principle of operation of (a) a gas filled detector, i.e. an ionization chamber; (b) a semiconductor detector, i.e. a silicon detector; and (c) a scintillation detector. The former two detectors are capacitors. The motion of charge results in an observable signal. The light of a scintillation detector is usually detected by a photomultiplier tube.

6.1.4. Detector requirements

The quality of a radiation detector is expressed in terms of sensitivity, energy, time and position resolution, and the counting rate a detector can handle. Obviously, other aspects such as cost, machinability and reliability are also very important. The latter will not be discussed in this chapter.

6.1.4.1. Sensitivity

In radiation detection, the sensitivity depends on (i) the solid angle subtended by the detector and (ii) the efficiency of the detector for interaction with the radiation. The first point will be obvious and is not discussed further. In nuclear medicine, relevant X ray and γ ray energies are in the range of ~30–511 keV. The detection efficiency is governed by the photoelectric effect and Compton scattering only. The attenuation length (in centimetres) of the

former is proportional to $\rho Z_{\text{eff}}^{3-4}$, where ρ is the density and Z_{eff} is the effective atomic number of the compound. Compton scattering is almost independent of Z; it is just proportional to ρ. The density of a gas filled detector is three orders of magnitude smaller than that of a solid state detector. Thus, solid state detectors are very important in nuclear medicine. At 511 keV, even the highest possible ρ and Z_{eff} are needed. Gas filled detectors are used in dosimetry.

6.1.4.2. Energy, time and position resolution

Energy, time and position resolution depend on a number of factors. These are different depending on the physical property considered and the type of detector; yet, there is one aspect in common. Resolution is strongly coupled to the statistics of the number of information carriers. For radiation energy E, this number is given by $N = E/W$ in which W is the mean energy needed to produce an information carrier. Typical W values are shown in Table 6.1. As the smallest number of information carriers in the process of signal formation is determinative, for scintillation the effect of the light sensor is also shown. From the W values, it can be seen that semiconductor detectors produce the largest number of information carriers and inorganic scintillators coupled to a photomultiplier tube (PMT) the smallest. If a γ ray energy spectrum is measured, the observed energy resolution is defined as the width of a line at half height (FWHM: full width at half maximum) ΔE divided by its energy E. With $N = E/W$, and ΔN being the corresponding FWHM:

$$\frac{\Delta E}{E} = \frac{\Delta N}{N} = 2.35\sqrt{\frac{FW}{E}}$$

(6.1)

where

ΔN is 2.35σ for a Gaussian distribution;
σ^2 is FN for the variance;

and F is the Fano factor. For gas filled detectors, $F = 0.05\text{–}0.20$, for semiconductors $F \approx 0.12$. For a scintillator, $F = 1$.

Using the corresponding F and W values, it can be seen from Eq. (6.1) that the energy resolution of a semiconductor is ~16 times higher than that of an inorganic scintillator PMT. In this discussion, other contributions to the energy resolution were neglected, viz. from electronic noise in the case of the semiconductor detector and from scintillator and PMT related effects in the

other case. Nevertheless, the large difference, by an order of magnitude, is characteristic of the energy resolutions.

TABLE 6.1.   MEAN   ENERGIES W TO   PRODUCE   INFORMATION CARRIERS

Detector type	W (eV)
Gas filled (electron–ion)	30
Semiconductor (electron–hole)	3
Inorganic scintillator (light quantum)	25
Inorganic scintillator + photomultiplier tube (electron)	100
Inorganic scintillator + silicon diode (electron–hole pair)	35

In nuclear medicine, time resolution is mainly of importance for PET. Time resolution depends primarily on two factors, the rise time and the height of the signal pulses. The effect of the former can be understood by considering that it is easier to measure the position of a pulse on a timescale with an accuracy of 100 ps if the rise time is 1 ns, than if it is 10 ns. The pulse height is important because there is noise as well. The higher the pulse relative to the noise, the easier it is to determine its position. In addition, time jitter due to pulse height (energy) variation will become less important. If time resolution is the issue, the fast response and fast rise time of inorganic scintillators and the fast response of the light sensors make the scintillator the preferred detector.

Position resolution can be obtained easiest by pixelating the detector at a pitch corresponding to the requested resolution. In nuclear medicine, position resolution is an issue in γ ray detection in the gamma camera and in single photon emission computed tomography (SPECT) and PET detection systems. In the latter, pixelated scintillators are used and the position resolution of a detector is determined by the pitch. More recently, studies have been published on the use of monolithic scintillator blocks in PET. Light detection occurs by means of pixelated sensors. In principle, this is analogous to the gamma camera. A relatively broad light distribution is measured using pixels that are smaller in size to define the centre of the distribution, thus obtaining a position resolution that is even better than the pixel size.

6.1.4.3. Counting rate and dead time

An achievable counting rate depends on (i) the response time of a detector, i.e. the time it takes to transport the charge carriers to form the signal or to emit

the scintillation light, and (ii) the time needed to process the signals and to handle the data. For a better understanding, the concept of dead time is introduced. It is the minimum time separation between interactions (true events) at which these are counted separately. Non-paralysable and paralysable dead time are considered. In the former case, if within a period of time τ after a true event a second true event occurs, it cannot be observed. If the second event occurs at a time $t > \tau$, it will be counted. The dead period is of fixed length τ. Defining true event rate T (number per unit time) and counting rate R, the fraction of time the system is dead is given by $R\tau$ and the rate of loss of events is $TR\tau$. Considering that the latter is also $T - R$, the non-paralysable case can be derived:

$$R = \frac{T}{1 + T\tau} \tag{6.2}$$

If in the paralysable model a second event occurs at $t > \tau$ after the first event, it will be counted. If a second event occurs at $t < \tau$ after the first event, it will not be counted. However, in the paralysable case, if $t < \tau$, the second event will extend the dead time with a period τ from the moment of its interaction. If a third event occurs at $t > \tau$ after the first event but within a period of time τ after the second event, it will not be counted either. It will add another period of τ. The dead time is not of fixed length. It can become much larger than the basic period τ and in this case it is referred to as 'extendable' dead time. Only if an event occurs at time $> \tau$ after the previous event will it be counted. In this case, the counting rate is the rate of occurrences of time intervals $>\tau$ between events, for which the following can be derived:

$$R = Te^{-T\tau} \tag{6.3}$$

Figure 6.2 demonstrates the relation between R and T for the two cases above and for the case of $\tau = 0$, i.e. $R = T$.

6.2. GAS FILLED DETECTORS

6.2.1. Basic principles

The mode of operation of a gas filled detector depends strongly on the applied voltage. In Fig. 6.3(a), the signal amplitude is shown as a function of the voltage V. If upon interaction with radiation an energetic electron ploughs through the gas, the secondary electrons produced will tend to drift to the anode and the ions to the cathode (see Fig. 6.1(a)). If the voltage is relatively low, the electric
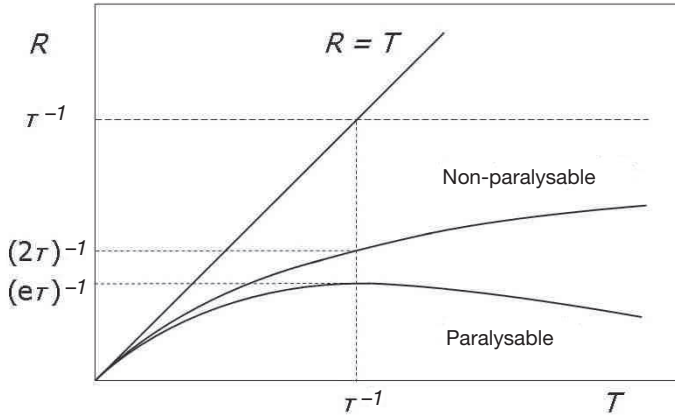
FIG. 6.2. Counting rate R as a function of true event rate T in the absence of dead time (R = T), in the non-paralysable case and in the paralysable case.

field E is too weak to efficiently separate the negative and positive charges. A number of them will recombine. The full signal is not observed — this is in the recombination region. Increasing the voltage, more and more electrons and ions escape from recombination. The region of full ionization is now reached. For heavier charged particles and at higher rates, this will happen at a higher voltage. The signal will become constant over a wide voltage range. Typical operating voltages of an ionization chamber are in the range of 500–1000 V.

For the discussion of operation at stronger electric fields, cylindrical detector geometry with a thin anode wire in the centre and a metal cylinder as cathode (see Fig. 6.3(b)) is introduced. The electric field $E(r)$ is proportional to the applied voltage V and inversely proportional to the radius r. At a certain voltage V_T, the threshold voltage, the electric field near the anode wire is so strong that a drifting electron will gain enough energy to ionize a gas atom in a collision. The proportional region is entered. If the voltage is further increased, the ionization zone will expand and an avalanche and significant gas amplification are obtained. At normal temperature and pressure, the threshold electric field $E_T \approx 10^6$ V/m. For parallel plate geometry with a depth of ~1 cm, this would imply that $V_T \approx 10$ kV, which is not practicable. Due to the r^{-1} dependence, in the cylindrical geometry, manageable voltages can be applied for proportional operation (1–3 kV). As long as the gas gain M is not too high ($M \approx 10^4$), it is independent of the deposited energy. This is referred to as the proportional region and proportional counter. If the voltage is further increased, space charge effects will start to reduce the effective electric field and, consequently, affect the gain. This process will start at a lower voltage for the higher primary ionization density events. The limited proportionality region is entered. With further increasing voltage, the pulse

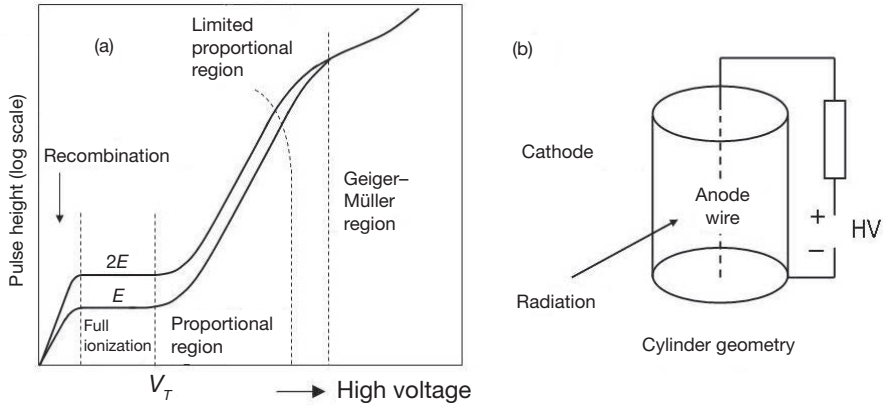height will eventually become independent of the deposited energy. This is the Geiger–Müller region.

FIG. 6.3. (a) Pulse height as a function of applied high voltage for gas filled detectors; (b) cylindrical detector geometry.

Instead of one wire in a cylindrical geometry, many equidistant parallel anode wires at a pitch of 1–2 mm can be positioned in a plane inside a box with the walls as cathode planes. This multiwire proportional chamber (MWPC) is employed in autoradiography. The technique of photo-lithography made it possible to introduce micro-patterned detectors that operate analogously to the MWPC. Examples are the micro-strip gas chamber and the gas electron multiplier. Spatial resolutions are of the order of 0.1 mm.

6.3. SEMICONDUCTOR DETECTORS

6.3.1. Basic principles

As shown in Fig. 6.1(b), a semiconductor detector is a capacitor. If upon interaction with radiation, electrons are lifted from the valence band into the conduction band, the transport of the charge carriers in an applied electric field is observed. However, if a voltage difference is supplied to electrodes on opposite sides of a slab of semiconductor material, in general, too high a current will flow for practical use as a detector. At room temperature, electrons are lifted from the valence band into the conduction band by thermal excitation due to the small gap ($E_{gap} \approx 1$ eV). The resulting free electrons and holes cause the current. A solution is found in making a diode of the semiconductor, operated in reverse bias. Silicon

is used as an example. The diode structure is realized by means of semiconductor-electronics technology. Silicon doped with electron-donor impurities, called n-type silicon, can be used to reduce the number of holes. Electrons are the majority charge carriers. Silicon with electron-acceptor impurities is called p-type silicon; the number of free electrons is strongly reduced. The majority charge carriers are the holes. When a piece of n-type material is brought into contact with a piece of p-type material, a junction diode is formed. At the junction, a space charge zone results, called a depletion region, due to diffusion of the majority charge carriers. When a positive voltage is applied on the n-type silicon side with respect to the p-type side, the diode is reverse-biased and the thickness of the depletion layer is increased. If the voltage is high enough, the silicon will be fully depleted. There are no free charge carriers left and there is virtually no current flowing. Only a small current will remain, the leakage or dark current.

To make a diode, n-type silicon is the starting material and a narrow zone is doped with impurities to make a p^+n junction, as indicated at the bottom of Fig. 6.1(b). The notation p^+ refers to a high doping concentration. For further reduction of the leakage current, high purity silicon and a blocking contact are used, i.e. an n^+ doping at the n-type side, also indicated in Fig. 6.1(b). If the leakage current is still problematic, the temperature can be decreased. The use of high purity semiconductor material is not only important for reducing the leakage current. Energy levels in the gap may trap charge carriers resulting from the interaction with radiation and the energy resolution of a detector would be reduced.

The above described approach is not the only way to make a detector. It is possible to start with p-type material and make an n^+p junction diode. Furthermore, it is possible to apply a combination of surface oxidation and deposition of a thin metal layer. Such contacts are called surface barrier contacts. If the thickness of a detector is <1 mm, it is even possible to use intrinsic silicon, symbol i, with p^+ and n^+ blocking contacts on opposite sides (p–i–n configuration). For thicker silicon detectors, yet another method is used. In slightly p-type intrinsic silicon, impurities are compensated for by introducing interstitial Li ions that act as electron donors. The Li ions can be drifted over distances of ~10 mm. Furthermore, if the bandgap of a semiconductor is large enough, just metal contacts will suffice.

Important parameters are the mobilities, μ_e and μ_h, and the lifetimes, τ_e and τ_h, of electrons and holes, respectively. The drift velocity $v_{e,h}$ in an electric field E is given by the product of the mobility and the field strength. Consequently, for a given detector size and electric field, the mobilities provide the drift times of the charge carriers and the signal formation times. From the mobilities and the lifetimes, information on the probability that the charge carriers will arrive at the

collecting electrodes is obtained. The path length a charge carrier can travel in its lifetime is given by:

$$\upsilon_{e,h}\tau_{e,h} = \mu_{e,h}\tau_{e,h}E \tag{6.4}$$

If this is not significantly longer than the detector depth, charge carriers will be lost.

6.3.2. Semiconductor detectors

Some properties of semiconductor detector materials of relevance for nuclear medicine, viz. the density ρ, effective atomic number for photoelectric effect Z_{eff}, E_{gap} and W value, the mobilities $\mu_{e,h}$ and the products of the mobilities, and the lifetimes of the charge carriers, are presented in Table 6.2.

Silicon is primarily of interest for (position sensitive) detection of low energy X rays, β particles and light quanta. The latter are discussed in Section 6.4.2.2.

TABLE 6.2. PROPERTIES OF SEMICONDUCTOR DETECTOR MATERIALS

	ρ (g/cm^3)	Z_{eff}	E_{gap} (eV)	W^a (eV)	Mobility (cm^2/Vs)		Mobility × lifetime (cm^2/V)	
					μ_e	μ_h	$\mu_e\tau_e$	$\mu_h\tau_h$
Si (300 K)	2.3	14	1.12	3.6	1 350	480	>1	~1
Si (77 K)			1.16	3.8	21 000	11 000	>1	>1
Ge (77 K)	5.3	32	0.72	3.0	36 000	42 000	>1	>1
CdTe (300 K)	6.2	50	1.44	4.7	1 100	80	3×10^{-3}	2×10^{-4}
Cd$_{0.8}$Zn$_{0.2}$Te (CZT-300 K)	~6	50	1.5–2.2	~5	1 350	120	4×10^{-3}	1×10^{-4}
HgI$_2$ (300 K)	6.4	69	2.13	4.2	70	4	5×10^{-3}	3×10^{-5}

[a] See Section 6.1.4.2.

For X ray detection in the range of ~300 eV to 60 keV, planar circular Li drifted p–i–n detectors — notated Si(Li) — are commercially available with a thickness up to 5 mm. Diameters are in the range of 4–20 mm. For typical field strengths of ~1000 V/cm, the drift times to the electrodes are on the order of tens of nanoseconds. Energy resolutions (FWHM) at 5.9 keV are ~130–220 eV if

operated at 77 K. Position sensitive silicon detectors with a large variety of pixel structures are commercially available. Silicon detectors are also used in personal dosimeters.

Germanium, with its higher density and atomic number, is the basic material for high resolution γ ray spectroscopy. Detectors are made of high purity material. Large volume detectors are made of cylindrical crystals with their core removed (coaxial geometry). High purity n-type or p-type is used with the corresponding junction contacts on the outside and the blocking contacts on the inside. Germanium detectors are operated at 77 K. Cylindrical detectors up to a diameter of ~10 cm and a height of ~10 cm are commercially available. Drift times to the electrodes can be as large as ~100 ns. Typical energy resolutions are ~1 keV at 122 keV γ ray energy and ~2 keV at 1332 keV.

Cadmium telluride (CdTe) and cadmium zinc telluride (CZT) are of interest because their atomic number is significantly higher than that of germanium, and room temperature operation is possible due to the larger bandgap. High purity n-type or p-type material is used. The energy resolution is worse than that of Ge detectors, e.g. 2.5% FWHM at 662 keV. This is primarily due to the relatively short lifetime of the holes, resulting in incomplete charge collection. Electronic correction techniques are used and/or detectors with special electrode configurations (small pixels or grids) are made to observe the electron signal only. Detector dimensions are up to approximately 25 mm × 25 mm × 10 mm. Detectors of 25 mm × 25 mm × 5 mm with 16 pixels × 16 pixels are available. These detectors are used, for example, for innovation of SPECT.

In principle, HgI_2 (mercury iodide) is an attractive material for efficient γ ray detection because of the large density and high atomic number. Owing to the relatively large bandgap, room temperature operation is possible. However, the mobilities are low and charge collection, in particular of the holes, is poor. Consequently, application is limited to detector thicknesses ≤10 mm. Field strengths of 2500 V/cm are applied and analogous to CdTe and CZT, methods are used to observe the electron signal only. Detector areas are up to ~30 mm × 30 mm.

6.4. SCINTILLATION DETECTORS AND STORAGE PHOSPHORS

6.4.1. Basic principles

Scintillation of a material is the prompt emission of light upon interaction with radiation. In nuclear medicine, inorganic ionic crystals are most important. They combine high density and atomic number with a fast response and a high light yield, and large crystals can be grown. These crystals form the backbone for

X ray and γ ray detection. Another group is formed by organic scintillators, viz. crystals, plastics and liquids, which have a low density and atomic number, and are primarily of interest for counting of β particles. In some inorganic scintillator materials, metastable states (traps) are created that may live from milliseconds to months. These materials are called storage phosphors. Scintillators and storage phosphors are discussed later in this section. However, as light detection is of paramount importance, light sensors are introduced first.

6.4.2. Light sensors

6.4.2.1. Photomultiplier tubes

The schematic of a scintillation detector is shown in Fig. 6.4(a). A scintillation crystal is coupled to a PMT. The inside of the entrance window of the evacuated glass envelope is covered with a photocathode which converts photons into electrons. The photocathode consists of a thin layer of alkali materials with very low work functions, e.g. bialkali K_2CsSb, multialkali $Na_2KSb:Cs$ or a negative electron affinity (NEA) material such as GaAs:Cs,O. The conversion efficiency of the photocathode η, called quantum efficiency, is strongly wavelength dependent (see Fig. 6.5). At 400 nm, $\eta = 25–40\%$. The emitted electrons are focused onto the first dynode by means of an electrode structure. The applied voltage is in the range of 200–500 V, and the collection efficiency $\alpha \approx 95\%$. Typical dynode materials are BeO–Cu, Cs_3Sb and GaP:Cs. The latter is an NEA material. If an electron hits the dynode, electrons are released by secondary emission. These electrons are focused onto the next dynode and secondary electrons are emitted, etc. The number of dynodes n is in the range of 8–12. The signal is obtained from the last electrode, the anode. At an inter-dynode voltage of ~100 V, the multiplication factor per dynode $\delta \approx 5$. In general, a higher multiplication factor is applied for the first dynode, e.g. $\delta_1 \geq 10$, to improve the single-electron pulse resolution, and consequently the signal to noise ratio. Starting with N photons in the scintillator and assuming full light collection on the photocathode, the number of electrons N_{el} at the anode is given by:

$$N_{el} = \delta_1 \delta^{n-1} \alpha \eta N \qquad (6.5)$$

Gains of 10^6–10^7 are obtained. A negative high voltage (1000–2000 V) is often used with the anode at ground potential and care must be taken of metal parts near the cathode. Furthermore, the detector housing should never be opened with the voltage on. Exposure to daylight would damage the photocathode permanently.
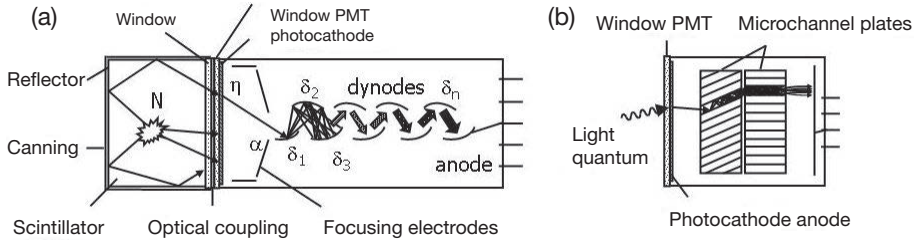
FIG. 6.4. (a) Schematic of a scintillation detector showing a scintillation crystal optically coupled to a photomultiplier tube (PMT); (b) schematic of a microchannel plate-photomultiplier tube.

PMTs are available with a large variety of specifications, including circular, square or hexagonal photocathodes. Cathode diameters are in the range of ~10 to ~150 mm. A ~50 mm diameter PMT has a length of ~150 mm including contact pins. Pixelated multi-anode PMTs exist as well. To optimize time resolution, special tubes are made with almost equal electron transit times to the anode, independent of the cathode position where an electron is emitted. Although the electron transit time is of the order of 30 ns, the transit time spread standard deviation is not more than ~250 ps, and the signal rise time ~1.5 ns.

A PMT aimed at ultra-fast timing is the microchannel plate (MCP)-PMT. For electron multiplication, it employs an MCP structure instead of a dynode configuration (see Fig. 6.4(b)). An MCP (thickness: ~1 mm) consists of a large number of closely packed hollow glass tubes (channel diameter: 5–50 μm). The inner surface of the tubes is covered with a secondary emission material, viz. PbO. The glass surfaces on the front and back side are covered with metal contacts. The MCP is placed in a vacuum, and a voltage of ~1000 V is applied between the contacts, positive on the back side. An electron that enters a glass tube on the front side will hit the wall and secondary emission will occur. The secondary electrons will be pulled to the back side by the electric field, hit the channel wall and produce secondaries, etc. Eventually, they will leave the tube at the back. Electron multiplication of $~10^4$ can be obtained. In an MCP-PMT, two MCPs are used at a close distance. The glass tubes are at an angle, thus preventing ions from gaining too much energy. This structure of two MCPs is called a chevron. At voltages of ~3000 V, stable gains of the order of 10^6 are obtained. The advantage of the MCP-PMT is the short path length of the electrons, resulting in transit times of a few nanoseconds and transit time spreads of ~100 ps. MCP-PMTs are commercially available with circular (~10 mm diameter) and square photocathodes, the latter with multi-anode structures. The sensitivities range from 115 nm (MgF_2 window) to infrared.
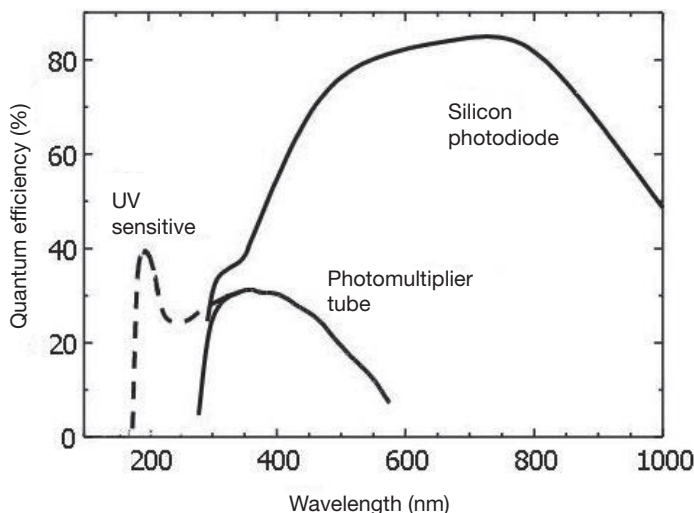
FIG. 6.5. *Quantum efficiency as a function of scintillation wavelength for a blue sensitive photomultiplier tube (full line), a photomultiplier tube with sensitivity extended into the ultraviolet (dashed extension) and a silicon photodiode.*

6.4.2.2. Silicon based photon sensors

Although PMTs are used on a large scale in nuclear medicine, the relatively large size, high voltages, small quantum efficiency and sensitivity to magnetic fields are a reason to prefer the use of silicon photodiodes in some applications. These diodes are usually of the p–i–n structure (PIN diodes). They have a thickness of ~2 mm including packaging, and are circular, rectangular or square, up to ~30 mm × 30 mm. Bias voltages are <150 V. The quantum efficiency of silicon diodes can be >80% at longer wavelengths (Fig. 6.5). The large capacitance of 20–300 pF, and leakage current, ~1–10 nA, are a disadvantage, resulting in a significant noise level that negatively affects energy resolution in spectroscopy.

An avalanche photodiode (APD) is the semiconductor analogue to the proportional counter. A high electric field is created in a small zone where a drifting electron can gain enough energy to produce an electron–hole (e–h) pair. An avalanche will result. The critical field for multiplication is ~10^7 V/m. The higher the voltage, the higher is the gain. Depending on the type, voltages are applied in the range of 50–1500 V. Gains are in the range of $M < 200$ to ~1000. The gain lifts the signal well above the noise as compared with the silicon diode. At a certain gain, the advantage is optimal. At very high electric fields, spontaneous charge multiplication will occur. The corresponding voltage is

called the break-down voltage V_{br}. For gains of $M \approx 10^5 - 10^6$, an APD can be used at voltages $>V_{br}$, where it operates in Geiger mode. The pulses are equal in magnitude. Signal quenching techniques have to be used. Circular and square APDs are available with areas in the sub-square millimetre to ~1 cm^2 range. Various pixelated APDs are available, e.g. of 4 pixels × 8 pixels at a pitch of ~2.5 mm and a fill factor ≤40%.

In a hybrid photomultiplier tube (HPMT), the photoelectrons are accelerated in an electric field resulting from a voltage difference of ~10 kV, applied between the photocathode and a silicon diode which is placed inside the vacuum enclosure. The diode is relatively small, thus reducing the capacitance and, consequently, the noise level. As the production of 1 e–h pair will cost 3.6 eV, ~3000 e–h pairs are produced in the diode per impinging electron. Consequently, the signals from one or more photons can be observed well separated. Equipped with an APD, an overall gain of ~10^5 is possible. HPMTs have been made with pixelated diodes. Window diameters are up to ~70 mm.

The silicon photomultiplier (SiPM) is an array of tiny APDs that operate in Geiger mode. The dimensions are in the range of ~20 μm × 20 μm to 100 μm × 100 μm. Consequently, the number of APDs per square millimetre can vary from 2500 to 100. The fill factor varies from <30% for the smallest dimensions to ~80% for the largest. The signals of all of the APDs are summed. With gains of $M \approx 10^5 - 10^6$, the signal from a single photon can be easily observed. By setting a threshold above the one electron response, spontaneous Geiger pulses can be eliminated. The time spread of SiPM signals is very small, <100 ps. Excellent time resolutions have been reported. Arrays of 2 pixels × 2 pixels and 4 pixels × 4 pixels of 3 mm × 3 mm, each at a pitch of 4 mm, have been commercially produced. A 16 pixel × 16 pixel array of 50 mm × 50 mm has recently been introduced. Blue sensitive SiPMs have a photon detection efficiency of ~25% at 400 nm, including a 60% fill factor.

6.4.3. Scintillator materials

6.4.3.1. Inorganic scintillators

In an inorganic scintillator, the bandgap has to be relatively large to avoid thermal excitation and to allow scintillation photons to travel in the material without absorption ($E_{gap} \geq 4$ eV). Consequently, inorganic scintillators are based on ionic-crystal materials. Three steps for the production of scintillation photons are considered (Fig. 6.6): (i) interaction of radiation with the bulk material and thermalization of the resulting electrons and holes — on the energy scale, electrons end up at the bottom of the conduction band and holes at the top of the valence band; (ii) transport of these charge carriers to intrinsic or dopant

luminescence centres; (iii) interaction with these centres, i.e. excitation, relaxation and scintillation. Using this model, the number of photons N_{ph} produced under absorption of a γ ray with energy E is:

$$N_{ph} = \frac{E}{\beta E_{gap}} SQ \qquad\qquad (6.6)$$

The first term on the right is the number of e–h pairs at the bandgap edge. Typically, $\beta \approx 2.5$. S and Q are the efficiencies of steps (ii) and (iii).
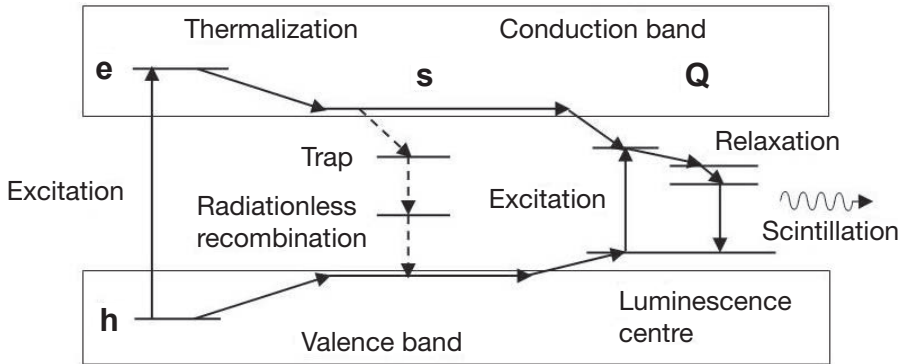

FIG. 6.6. Energy diagram showing the main process steps in an inorganic scintillator.

For the most relevant scintillators, the wavelength at emission maximum λ_{max}, light yield N_{ph}, best reported energy resolution at 662 keV R_{662} and the decay time of the scintillation pulse τ are presented in the last four columns of Table 6.3. In the first columns, some material properties are given, namely density, effective atomic number for photoelectric effect Z_{eff}, attenuation length at 511 keV, $1/\mu_{511}$, and the percentage of interaction by the photoelectric effect at 511 keV. These scintillators are commercially available. If hygroscopic, they are canned with reflective material (Fig. 6.4). Only BaF_2 and BGO have an intrinsic luminescence centre. The other scintillators have Tl^+ or Ce^{3+} ions as dopant luminescence centre. The cerium doped scintillators show a relatively fast response of the order of tens of nanoseconds due to the allowed 5d → 4f dipole transition of the Ce ion. The transitions of the Tl doped scintillators are forbidden and are, consequently, much slower. In general, mixed or co-doped crystals have advantages for crystal growing, response time, light yield or afterglow effects. Large variation is observed for light yields. This is mainly due to $S < 1$, i.e. there are traps of different kinds, resulting in loss of e–h pairs by non-radiative

transitions. Using Eq. (6.6) and the proper values of E_{gap}, only $LaBr_3$:Ce appears to have $S \approx Q \approx 1$.

TABLE 6.3. SPECIFICATIONS OF SOME INORGANIC SCINTILLATORS

Scintillator	ρ (g/cm^3)	Z_{eff}	$1/\mu_{511}$ (mm)	Photoelectric effect (%)	λ_{max} (nm)	N_{ph} (photons/MeV)	R_{662} (%)	τ (ns)
NaI:Tl[a]	3.67	51	29	17	410	41 000	6.5	230
CsI:Tl	4.51	54	23	21	540	64 000	4.3	800, 10^4
BaF$_2$	4.88		23		220 310	1 500 10 000		0.8 600
Bi$_3$Ge$_4$O$_{12}$ (BGO)	7.1	75	10.4	40	480	8 900		300
LaCl$_3$:Ce[a]	3.86	49.5	28	15	350	49 000	3.3	25
LaBr$_3$:Ce[a]	5.07	46.9	22	13	380	67 000	2.8	16
YAlO$_3$:Ce (YAP)	5.5	33.6	21	4.2	350	21 000	4.4	25
Lu$_{0.8}$Y$_{0.2}$Al:Ce (LuYAP)	8.3	65	11	30	365	11 000		18
Gd$_2$SiO$_5$:Ce (GSO)	6.7	59	14.1	25	440	12 500	9	60
Lu$_2$SiO$_5$:Ce,Ca (LSO)	7.4	66	11.4	32	420	~36 000	7	36–43
Lu$_{1.8}$Y$_{0.2}$SiO$_5$: Ce (LYSO)	7.1		12		420	30 000	7	40

[a] Hygroscopic.

6.4.3.2. Organic scintillators — crystals, plastics and liquids

The scintillation mechanism of organic scintillators is based on molecular transitions. These are hardly affected by the physical state of the material. There are pure organic scintillator crystals such as anthracene, plastics such as polystyrene, and liquids such as xylene. Furthermore, there are solutions of organic scintillators in organic solid (plastic) and liquid solvents. Typical combinations are p-terphenyl in polysterene (plastic) and p-terphenyl in toluene. There are also systems with POPOP (para-phenylene-phenyloxazole) added for wavelength shifting. In general, organic scintillators luminesce at ~420 nm, have

a light yield of ~10 000 photons/MeV of absorbed γ ray energy and the decay times are about 2 ns. The scintillators are usually specified by a commercial code.

6.4.3.3. Storage phosphors — thermoluminescence and optically stimulated luminescence

A storage phosphor is a material analogous to an inorganic scintillator. The difference is that a significant part of the interaction energy is stored in long-living traps. These are the memory bits of a storage phosphor. The lifetime must be long enough for the application considered. Readout is done either by thermal stimulation (heating) or by optical stimulation. An electron is lifted from the trap into the conduction band and transported to a luminescence centre. The intensity of the luminescence is recorded. These processes have been coined thermoluminescence and optically or photon stimulated luminescence. Storage phosphors have been used for dosimetry for more than fifty years (thermoluminescence dosimeter). In particular, LiF:Mg,Ti (commercial name TLD-100) is widely used. The sensitivity is in the range of ~50 μGy to ~1 Gy. A newer and more sensitive material is LiF:Mg,Cu,P (GR-200), with a sensitivity in the 0.2 μGy to 1 Gy range. Recently, an optically stimulated luminescent material has been introduced, Al_2O_3:C. The sensitivity is in the range of 0.3 μGy to 30 Gy. Storage phosphors are also used in radiography.

BIBLIOGRAPHY

INTERNATIONAL CONFERENCE ON INORGANIC SCINTILLATORS AND THEIR APPLICATIONS, SCINT 2007, IEEE Trans. Nucl. Sci. **55** (2008) 1029–1564.

— SCINT 2009, IEEE Trans. Nucl. Sci. **57** (2010) 1157–1520.

INTERNATIONAL WORKSHOP ON ROOM-TEMPERATURE SEMICONDUCTOR X- AND GAMMA-RAY DETECTORS (15th workshop), IEEE Trans. Nucl. Sci. **54** (2007) 761–880.

— (16th workshop), IEEE Trans. Nucl. Sci. **56** (2009) 1697–1884.

KNOLL, G.F., Radiation Detection and Measurement, 4th edn, John Wiley & Sons, New York (2010).

LEO, W.R., Techniques for Nuclear and Particle Physics Experiments, 2nd edn, Springer, Berlin (1994).

PROCEEDINGS OF NUCLEAR SCIENCE SYMPOSIUM AND MEDICAL IMAGING CONFERENCE (annually), IEEE Trans. Nucl. Sci. (recent volumes).

RODNYI, P.A., Physical Processes in Inorganic Scintillators, CRC Press, Boca Raton, FL (1997).

SCHLESINGER, T.E., JAMES, R.B. (Eds), Semiconductors for Room Temperature Nuclear Detector Applications, Academic Press, San Diego, CA (1995).

TAVERNIER, S., GEKTIN, A., GRINYOV, B., MOSES, W.M. (Eds), Radiation Detectors for Medical Applications, Springer, Dordrecht, Netherlands (2006).